Author's personal copy

Available online at www.sciencedirect.com
ScienceDirect
Scripta Materialia 63 (2010) 1224–1227
Scripta MATERIALIA
www.elsevier.com/locate/scriptamat

Direct observations of silver nanoink sintering and eutectic remelt reaction with copper

John W. Elmer[a,*] and Eliot D. Specht[b]

[a]Lawrence Livermore National Laboratory, Livermore, CA 94550, USA
[b]Oak Ridge National Laboratory, Oak Ridge, TN 37831, USA

Received 31 July 2010; revised 21 August 2010; accepted 22 August 2010
Available online 27 August 2010

Ag nanoink sintering kinetics and subsequent melting is studied using in situ synchrotron-based X-ray diffraction. Direct observations of Ag nanoink sintering on Cu demonstrate its potential for materials joining since the Ag nanoink sinters at low temperatures but melts at high-temperatures. Results show low expansion coefficient of sintered Ag, nonlinear expansion as Ag densifies and interdiffuses with Cu above 500 °C, remelting consistent with bulk Ag, and eutectic reaction with Cu. The results demonstrate the usefulness of Ag nanoink as a high-temperature bonding medium.
© 2010 Acta Materialia Inc. Published by Elsevier Ltd. All rights reserved.

Keywords: Nanoink; Brazing; In situ X-ray diffraction; Interdiffusion; Lattice expansion

Microelectronics applications are being developed for the direct writing of electrically conductive fine wiring for lower-cost alternatives to conventional photolithography. One of the more promising direct writing techniques uses nanoinks that contain nanometer-sized metallic particles suspended in an organic dispersant fluid [1,2]. The nanoparticles sinter at much lower temperatures than their conventional counterparts due to their high surface area to volume ratio and small radius of curvature, which reduces their melting points and increases diffusion rates drastically below their bulk values [3]. Silver, for example, has a bulk melting temperature of 962 °C, but will locally melt at temperatures around 200 °C for particle sizes less than 20 nm [2,4]. Silver nanopastes (high viscosity) and nanoinks (low viscosity) with these properties are available from multiple sources [5] and are being considered for materials joining concepts in addition to microelectronic circuits [6]. Nanoinks are currently being developed from Cu [7] as a lower-cost alternative to more noble Ag and Au [8], and from Sn-based alloys as lower melting point alternatives for lead-free solder applications [9].

The unusually low melting and sintering temperatures of nanoparticulate inks and pastes can be used for materials joining since they sinter at low temperatures but have high melting temperatures after the initial sintering [4,6,9]. Low-temperature sintering allows joints to be made at low temperatures, which is highly desirable when joining temperature-sensitive components. The high melting temperature allows subsequent joints to be made at the same, or even higher temperatures, for multiple joining sequences and repair work, which are often required in microelectronic packaging. One drawback is that nanoinks require organic surfactants to disperse the nanoparticles and keep them from agglomerating at room temperature [2]. These dispersants need to be removed in order for sintering to take place, and this is usually done using a thermal processing method. The thermal treatment generally requires temperatures in excess of 150 °C to remove the organic dispersants [2], and is usually conducted using bulk heating methods, although flash heating has also been explored [10].

Although a significant amount of work has been performed to demonstrate the useful properties of nanoinks for direct writing and joining, little work has been performed to demonstrate the high melting temperature, or the ability to use nanoinks as indirect eutectic bonding media. In this paper, silver nanoink is studied using in situ synchrotron-based X-ray diffraction to follow the kinetics of the initial sintering step, and to demonstrate the ability to the silver nanoink to be used at high-temperatures. In addition, the silver nanoink is explored as a possible eutectic bonding medium with copper as a less expensive alternative to physical vapor deposition or electroplating methods.

* Corresponding author. Tel.: +1 925 422 6543; fax: +1 925 423 7040; e-mail: elmer1@llnl.gov

1359-6462/$ - see front matter © 2010 Acta Materialia Inc. Published by Elsevier Ltd. All rights reserved.
doi:10.1016/j.scriptamat.2010.08.044

Author's personal copy

In situ X-ray diffraction experiments were conducted on Ag nanoink by heating and cooling a Cu substrate coated with the nanoink under controlled conditions while simultaneously performing X-ray diffraction in real-time. These experiments were performed at the Advanced Photon Source (APS), using the UNICAT beam line BM-33-C with X-ray beam energies of 27.9 keV ($\lambda = 0.4476$ nm) from a ring current of 100 mA. The X-ray beam line was set up with a water-cooled Si (1 1 1) monochromator, and the beam was focused and sized to dimensions of approximately 2 mm wide by 0.5 mm high using a dynamically bent Si crystal and collimator slits. The diffracted beams are detected with a 2048 × 2048 pixel areal detector placed downstream from the sample, and the diffraction patterns were acquired every 2 s using a 1 s integration time. Additional details about this X-ray beam line can be found elsewhere [11,12].

The nanoink used in the experiments was produced by Harima and is designated NPS-J. It is composed of 53–58 mass% Ag in tetradecane, with a reported mean particle size of 5 nm and a range of sizes between 3 and 7 nm. The nanoink has a reported viscosity of 8.4 mPa s, and a volume of 10–16% after curing at a recommended sintering temperature of 220 °C. The nanoink was placed on high-purity oxygen-free high-conductivity Cu substrates using a syringe to apply one drop to the 5.3 mm diameter Cu substrate where it quickly wet the surface. The in situ experiments were performed by placing the Cu sample with the nanoink deposit into a graphite heater, and then placing the heater into the water-cooled grips of the heating stage with a ~5° tilt to the axis of the X-ray beam. This same heating technique has been described for previous work with similar synchrotron-based experiments [11,12]. The Cu substrate was aligned in the graphite heater so that the 2 mm × 0.5 mm X-ray beam was centered on the surface of the Cu sample to observe reactions with the nanoink. The sintering operation was first performed by heating the sample in air while simultaneously performing X-ray diffraction to determine the kinetics of the sintering process. Once the sintering was complete, an environmental chamber was placed over the sample holder stage and evacuated to approximately 10 mTorr using a turbomolecular pump. The Ag–Cu eutectic reaction was performed next, in vacuum to prevent oxidation of the sintered silver, during heating to high-temperatures. In situ X-ray diffraction patterns were collected in real-time throughout the experiment and analyzed later to observe the phase transformations that occurred during sintering and heating to elevated temperatures.

The recommended nanoink sintering profile requires heating in air at 220 °C for approximately 60 min. This heat treatment is sufficient to completely burn off the organic dispersants and subsequently sinter the nanoparticles into a solid layer [6]. The fraction of solid remaining after sintering Harima NPS-J Ag nanoink is approximately 0.15 of the original volume, which results in a sintered Ag layer approximately 3 μm thick. This thin layer of Ag allows the high-energy synchrotron beam (27.9 kV) to penetrate completely through it and into the Cu substrate below, producing diffraction peaks from both metals during sintering.

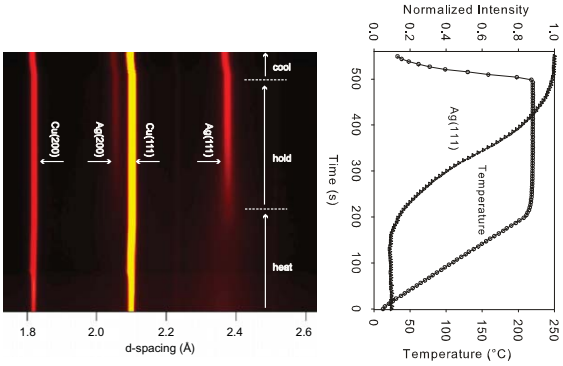

Figure 1. Sintering cycle for the Ag nanoink at 220 °C. In situ X-ray diffraction patterns are plotted in pseudocolor on the left, with corresponding temperature profile and normalized peak intensity (maximum counts = 4429) for the Ag on the right.

The results of the nanoink sintering at 220 °C are summarized in Figure 1. The in situ X-ray diffraction patterns in pseudocolor are shown on the left; lighter colors correspond to higher-intensity peaks. The diffraction patterns are plotted sequentially from the beginning of heating ($t = 0$ s) to the end of the experiment after cooling ($t = 570$ s). Two diffraction peaks each are present in the d-spacing window of 1.8–2.4 Å, representing the face-centered cubic (fcc) (1 1 1) and the (2 0 0) planes of both Ag and Cu. The right side of the figure shows the corresponding temperature profile, indicating that the sample was heated at a rate of 1 °C s^{-1}, and held isothermally at 220 °C for 5 min prior to being rapid cooled back to room temperature. In addition, the normalized intensities of the Ag (1 1 1) peaks were measured using diffraction peak-fitting software, and the results are also plotted in Figure 1.

The main result of the sintering experiment is the sharpening of the Ag diffraction peaks, from something very diffuse at low temperatures to sharp peaks that form during the isothermal hold. During this transition, the intensity of the Cu peaks remain relatively constant in comparison. The results show that the Ag peak increases intensity by an order of magnitude during sintering, from a normalized peak intensity of 0.096 (424 counts) to 1.0 (4429 counts) at the end of the experiment. Almost all of the increase in intensity of the diffraction peak occurs after the isothermal hold of 220 °C is attained, and the trend of the peak intensity with time during the isothermal hold follows a sigmoidal shape. Based on this data it appears as though a 5 min hold time at 220 °C is sufficient to sinter the NPS-J nanoink into a stable configuration. Additional experiments are planned as future work to determine the kinetics of the sintering process at different temperatures.

Nanoink deposits are reported to have properties similar to bulk material after sintering. For example, electrical resistivity is reported to be within 2–3× bulk values [10], and melting temperatures are assumed to be equal to bulk values [6]. Resistivities of the sintered deposits are frequently studied for their use in microelectronics applications; however, demonstration of the high melting temperature has not been performed in detail. In order to verify the high melting temperature, the previ-

Author's personal copy

ously sintered Ag deposit on the Cu substrate was reheated in vacuum to 815 °C while simultaneously performing in situ X-ray diffraction. This temperature is above the Ag–Cu eutectic temperature of 780 °C [13], to demonstrate the high-temperature stability of the Ag sintered deposit, and to demonstrate the ability of nanoinks to be used for high-temperature eutectic soldering or brazing.

The results of the reheating experiment are presented in Figure 2. As before, the in situ X-ray diffraction patterns are shown on the left with the diffraction patterns plotted sequentially from the beginning of heating ($t = 0$ s) to the end of the experiment after cooling ($t = 730$ s). The same two diffraction peaks are shown representing the fcc (1 1 1) and the (2 0 0) planes of Ag and Cu. The right side of the figure shows the corresponding temperature profile, indicating that the sample was rapidly heated at a rate of 10 °C s^{-1} to 815 °C, where it was held for approximately 30 s prior to being rapidly cooled back to room temperature. The intensity of the Ag (1 1 1) peaks were measured using diffraction peak-fitting software, and the results are also plotted in Figure 2.

The Ag (1 1 1) and Cu (1 1 1) diffraction peaks are more intense than the Ag (2 0 0) and Cu (2 0 0) planes, but otherwise show similar features, so only the (1 1 1) planes will be discussed. In the case of Ag, the intensity of the initial normalized diffraction pattern is 0.54 (4429 counts), which is nominally the same value as after the sintering experiment. This value increases to 1.0 (8286 counts) at the end of the remelting experiment. A large fraction of the increase in the Ag (1 1 1) peak intensity occurs during heating, and does so only after the temperature passes above the sintering temperature of 220 °C. This initial increase in the intensity of the Ag (1 1 1) peaks results in a rise to 0.75 (6190 counts), which is nearly 2× that after sintering at 220 °C. The increase in peak intensity indicates that sintering was not completed at 220 °C during the 5 min hold, and that higher temperatures create a more highly sintered Ag layer. The Ag diffraction peaks are present all the way up to a temperature of 789 °C, where a rapid drop in intensity occurs as the main Ag (1 1 1) peaks disappear. The disappearance of these peaks indicates that melting does occur but not until the temperature has reached the Ag–Cu eutectic temperature of 780 °C where Ag and Cu interdiffuse to create the eutectic alloy.

Careful examination of the diffraction peaks show that not all of the Ag melts at the same temperature. Evidence for this is indicated by the small diffraction peak that tails off of the main Ag (1 1 1) peak. This tail, indicated by the starred arrow in Figure 2, is most likely Ag on the top surface of the sample that is furthest away from the Cu, and required additional time to interdiffuse with Cu to create the eutectic composition. The intensities of the Ag (1 1 1) peak in the tail are indicated by the solid circles, and eventually disappear as the sample is held at 815 °C. Once the heater is shut off, the sample solidifies and cools at an initial rate of approximately 10 °C s^{-1}. The measured solidification temperature is 769 ± 20 °C, which indicates that the sample solidified close to the eutectic temperature. Accompanying solidification is a rapid increase in the Ag diffraction peaks to a normalized intensity of about 0.6 (7249 counts), which increase to 1.0 (8286 counts) as the sample cools to room temperature.

The results of the reheating experiment clearly show that the sintered Ag nanoink withstands temperatures all the way to the Ag–Cu eutectic temperature of 780 °C, which is consistent with the sintered Ag having bulk melting temperature if it had not reacted with the Cu substrate. In addition, the ability of the sintered Ag deposit to react with Cu and melt at the eutectic temperature demonstrates the possibility of using nanoinks as indirect soldering and brazing mediums.

The diffraction patterns shown in Figure 2 indicate that the Ag peaks disappear during melting, but that the Cu peaks remain throughout the entire experiment. The presence of the Cu peaks indicates that the melt layer is thin enough to allow the X-rays to pass through it and into the underlying Cu substrate below. Further analysis of the diffraction peaks shown in Figure 2 for the reheating experiment was performed to determine the Ag lattice parameter.

The results are presented in Figure 3, which plots the lattice parameter, a_o, for Ag based on the (1 1 1) planes. During heating the lattice parameter increases approximately linearly up to a temperature of 500 °C, where it levels off before decreasing with increasing temperature at 650 °C. The decrease in the lattice parameter is caused by interdiffusion of Cu into the Ag layer due to the smaller lattice parameter of Cu (3.608 Å) than Ag (4.086 Å)

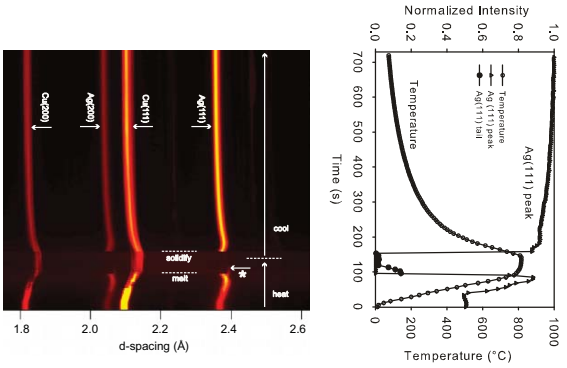

Figure 2. Reheat cycle of the sintered Ag deposit. In situ X-ray diffraction patterns are plotted in pseudocolor on the left, with the corresponding temperature profile and normalized peak intensity (maximum counts = 8286) for the Ag on the right.

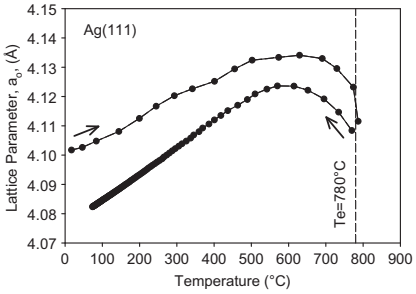

Figure 3. Lattice parameters for sintered Ag on heating and cooling to 815 °C. Melting occurs at the Ag–Cu eutectic temperature, *T*e, of 780 °C. Arrows indicate the direction of heating and cooling.

Author's personal copy

Table 1. Summary of the CTEs for Ag on heating and cooling for the (1 1 1) and (2 0 0) planes.

Temperature range	Silver CTE (ppm °C−1)		
	Ag (1 1 1)	Ag (2 0 0)	Avg.
25–500 °C (heating)	15.9	15.8	15.9
500–25 °C (cooling)	22.1	22.0	22.0

[14]. The Ag peaks reappear on solidification, and the process is reversed with the lattice parameter increasing during cooling to a temperature of about 650 °C, and then decreasing after that to room temperature. The reversal of the nonlinear expansion behavior on cooling is related to the higher solubility of Cu in Ag at elevated temperatures: 14 at.% at 780 °C vs. less than 0.1 at.% at room temperature [13]. During cooling, a Cu-rich phase separates from the Ag–Cu alloy, which increases the lattice parameter of the remaining Ag–Cu alloy. The separation of Cu from Ag requires thermally activated diffusion to take place which is not sustained at temperatures below about 500 °C for the cooling rate of 10 °C s^{-1}, resulting in typical contraction behavior at lower temperatures. A net decrease in the Ag lattice parameter from approximately 4.10–4.08 Å occurs during the reheating and cooling cycle due to the remnant Cu in the Ag film.

The coefficient of thermal expansion (CTE) of the sintered Ag deposit was measured both during heating, and during cooling after eutectic melting, for the Ag (1 1 1) and Ag (2 0 0) planes. These results are summarized in Table 1 for a temperature range of 25–500 °C, which is in the linear portion of the observed expansion curves. The measured CTE on heating of 15.9 ppm $°C^{-1}$ is considerably less than that on cooling of 22.0 ppm $°C^{-1}$. The reported CTE of Ag is 22.1 ppm $°C^{-1}$ over this temperature range [15], which is close to the value on cooling. The low CTE measured on heating is most likely due to the Ag sintered film not being fully dense. Lattice expansion has been reported for nanocrystalline Cu, Nb and Ni, relative to microcrystalline or single-crystal values, and has been attributed either to surface tension, expanded grain boundaries or vacancies [16–18]. If a similar effect occurs in Ag, a lattice contraction would occur as grains grow with increasing temperature, accounting for the reduced CTE on heating.

In summary, the following conclusions can be made:

1. Synchrotron-based X-ray diffraction can be used to study real-time sintering kinetics of nanoinks and subsequent phase transformations that occur between nanoinks and corresponding substrates.
2. In situ X-ray diffraction during sintering/curing at 220 °C showed that the initial diffuse Ag diffraction peaks of the nanoink narrowed and increased in intensity in a nonlinear way with holding time. The sintering behavior followed a sigmoidal relationship and appeared to be near completion after 5 min at this temperature.
3. In situ X-ray diffraction during reheating of the sintered Ag deposit on Cu showed that the Ag continued to sinter at temperatures above the initial curing temperature, and showed no signs of melting up to the eutectic temperature between Ag and Cu at 780 °C. Reaction with the Cu substrate and melting at this temperature demonstrates that Ag nanoinks can be used as a eutectic bonding medium.
4. In situ measurements of the lattice parameter of the Ag sintered deposit revealed a CTE on heating of 15.9 ppm $°C^{-1}$, which is lower than the bulk value of 22.1 ppm $°C^{-1}$.
5. Interdiffusion of Cu into the Ag layer occurred at temperatures higher than 500 °C which reduced its lattice parameter and resulted in highly nonlinear lattice expansion behavior of Ag.

The authors would like to thank Jenia Karapetrova of the APS for assisting with the synchrotron beam-line setup and operation. This work was performed under the auspices of the US Department of Energy by Lawrence Livermore National Laboratory under Contract DE-AC52-07NA27344, and by Oak Ridge National Laboratory under Contract DE-AC05-00OR22725. The ORNL portion of this work was fully supported by the Materials Sciences and Engineering Division, Office of Basic Energy Sciences, US Department of Energy. The in situ synchrotron experiments were performed on 34-BM-C at the APS, which is supported by the US DOE, Basic Energy Sciences, Office of Science under contract No. W-31-109-ENG-38.

[1] W. Peng, V. Hurskainen, S. Dunford, S. Quander, R. Vatanparast, in: IEEE 55th Electronic Components and Technology Conference Proceedings, 2005, pp. 77–82.
[2] D. Wakuda, K.-S. Kim, K. Suganuma, IEEE Trans. Compon. Packag. Tech. 32 (3) (2009) 627–632.
[3] Ph. Buffat, J.-P. Borel, Phys. Rev. A 13 (6) (1976) 2287.
[4] M. Maruyama et al., Appl. Phys. A 93 (2008) 467–470.
[5] A. Suzuki et al., Rev. Sci. Instrum. 76 (2005) 023907.
[6] A. Hirose, K.F. Kobayashi, in: Y.N. Zou (Ed.), Microjoining and Nanojoining, Woodhead Publishing, Cambridge, 2008, pp. 250–268.
[7] T. Bakhisheva, V. Subramanian, J. Electron. Mater. 38 (12) (2009) 2720.
[8] S. Jeong et al., Adv. Funct. Mater. 18 (2008) 679–686.
[9] C. Anderson, C. Zou, B. Yang, Y. Gao, J. Liu, Q. Zhai, IEEE 2nd Electronics System Integration Technology Conference, Greenwich, UK, 2008, p. 915.
[10] H.-S. Kim, S.R. Dhage, D.-E. Shim, H.T. Hahn, Appl. Phys. A 97 (2009) 791–798.
[11] J.W. Elmer, E.D. Specht, M. Kumar, J. Electron. Mater. 39 (3) (2010) 273–282.
[12] J.W. Elmer, T.A. Palmer, E.D. Specht, J. Vac. Sci. Technol., A 24 (4) (2006) 978–987.
[13] Binary Alloy Phase Diagrams, second ed., vol. 2, ASM International, Materials Park, OH, 1990.
[14] Pearson's Handbook of Crystallographic Data for Intermetallic Phases, desk ed., vol. 2, ASM International, Materials Park, OH, 1997.
[15] ASM Metals Handbook, ninth ed., vol. 2, ASM International, Materials Park, OH, 1979.
[16] R. Banerjee, E.A. Sperling, G.B. Thompson, H.L. Fraser, S. Bose, P. Ayyub, Appl. Phys. Lett. 82 (24) (2003) 4250–4252.
[17] Y. Champion, F. Bernard, N. Millot, P. Perriat, Appl. Phys. Lett. 23 (2005) 1947887.
[18] M.Y. Gamarnik, Phys. Status Solidi B – Basic Res. 168 (2) (1991) 389–395.